Dissolution of silicate minerals and nutrient availability for corn grown successively

Abstract – The objective of this work was to evaluate the nutrient availability for corn (*Zea mays*) grown successively in pure and ground biotite schist and biotite syenite rock samples. The rock powders were subjected to chemical, physical, and mineralogical characterization, and the availability of the elements released to the plants was determined. Plant and rock materials were evaluated at the end of seven successive growth cycles. Biotite schist and biotite syenite provided nutrients – as K, Ca, Mg, Fe, and Mn – to the corn plants. The nutrients accumulated in plant tissues came mostly from minerals containing oxidizable Fe and Mn in their structure, such as biotite, chlorite, and clinopyroxene. The congruent dissolution of some of the fine particles of these minerals, solubilize elements, which may, then, be available to the plants.

Index terms: agromineral, biotite, bioweathering, congruent dissolution, nutrient availability.

Luise Lottici Krahl[1] (iD),
Leonardo Fonseca Valadares[2] (iD),
José Carlos Sousa-Silva[3] (iD),
Giuliano Marchi[3 ✉] (iD) and
Éder de Souza Martins[3] (iD)

[1] Universidade de Brasília, Campus de Planaltina, Área Universitária, nº 01, Vila Nossa Senhora de Fátima, CEP 73345-010 Planaltina, Brasília, DF, Brazil.
E-mail: luisekrahl@yahoo.com.br

[2] Embrapa Agroenergia, Parque Estação Biológica, s/nº, Edifício Embrapa Agroenergia, Caixa Postal 40.315, CEP 70770-901 Brasília, DF, Brazil.
E-mail: leonardo.valadares@embrapa.br

[3] Embrapa Cerrados, Rodovia BR-020, Km 18, Caixa Postal 08223, CEP 73310-970 Planaltina, DF, Brazil.
E-mail: jose.sousa-silva@embrapa.br, giuliano.marchi@embrapa.br, eder.martins@embrapa.br

✉ Corresponding author

Dissolução de minerais silicáticos e disponibilidade de nutrientes para milho cultivado sucessivamente

Resumo – O objetivo deste trabalho foi avaliar a disponibilidade de nutrientes para milho (*Zea mays*) cultivado sucessivamente em amostras das rochas puras e moídas biotita xisto e biotita sienito. Os pós das rochas foram submetidos à caracterização química, física e mineralógica, e a disponibilidade dos elementos liberados para as plantas foi determinada. Os materiais de planta e rocha foram avaliados no final de sete ciclos sucessivos de cultivo. A biotita xisto e a biotita sienito forneceram nutrientes – como K, Ca, Mg, Fe e Mn – para as plantas de milho. Os nutrientes acumulados no tecido das plantas vieram de minerais contendo Fe e Mn oxidáveis em sua estrutura, tais como biotita, clorita e clinopiroxênio. A dissolução congruente de algumas partículas finas dos minerais, solubiliza elementos que podem, então, ser disponibilizados para as plantas.

Termos para indexação: agromineral, biotita, biointemperismo, dissolução congruente, disponibilidade de nutrientes.

Introduction

Although the weathering of silicate minerals is considered a slow process, certain rock minerals might weather in a shorter time than expected, especially when ground rocks interact with the plant rhizosphere (Manning et al., 2017; Basak, 2019; Ciceri & Allanore, 2019). Several studies have been carried out to evaluate the ability of

different silicate minerals to provide nutrients to plants in the short-term, evidencing both the incongruent (solids + dissolved products) and the congruent (complete) dissolution of micas and of finer fractions of minerals, respectively (Hinsinger et al., 1993; Li et al., 2015; Manning et al., 2017; Ciceri et al., 2019).

Under plant-induced weathering, the dissolution rates of minerals may vary depending on the minerals it contains, grinding process, and plant species. The role of the plant is related to its root activity, the release of organic substances, and associated microbial populations (Li et al., 2014; Bray et al., 2015; Burghelea et al., 2015). Other factors also affect the dissolution of minerals in natural conditions, among which stand out: the area of exposure of the minerals; and chemical reactions, especially acid-base, oxidation-reduction, and adsorption-desorption-precipitation. Element absorption and release by different species of plants and organisms, as well as chelates and temperature and humidity, are also important in this dynamic process.

Faster dissolution rates are observed in minerals characterized by: low concentrations of aluminum and silicon in their structure; a high content of oxidizable iron and manganese; and alkali and alkaline earth cations, including potassium, calcium, and magnesium (Li et al., 2014; Bray et al., 2015; Burghelea et al., 2015). During the grinding process, it is possible that particles undergo a selection process producing materials with a composition different from that of the original rock, highlighting a by-product – fine powder – of gravel production, obtained by the breakage of particles at its weakest cleavage plane, where easily weathered minerals are undergoing a continuous selection process.

The incongruent dissolution may lead to the production of secondary or clay minerals – such as illite or hydrous mica, vermiculite, chlorite, and interstratified minerals – due to mineral alteration through cation release (Naderizadeh et al., 2010; Norouzi & Khademi, 2010). Although mostly incongruent, the dissolution rate of the biotite minerals found in rocks, as schists and syenites, is relatively fast, which is indicative that these rocks can be a suitable potassium source for plants (Burghelea et al., 2015; Li et al., 2015; Manning et al., 2017).

The uptake of potassium from silicate minerals varies depending on plant species. The reserves of this element in the soil have been shown to be better exploited, in general, by monocotyledons, such as gramineous species, which developed a very efficient mechanism for iron mobilization during their evolution, when compared with that of dicotyledons (Broadley et al., 2012). In addition, for some plants, root-induced release of the interlayer potassium occurred after only a few weeks of growth (Hinsinger et al., 1992; Wang et al., 2000; Norouzi & Khademi, 2010; Li et al., 2015).

Nowadays, the research have been focused on the release of potassium from minerals. The potassium-rich minerals present in silicate rocks – such as micas and K-feldspars and their weathering products – provide a significant amount of the potassium required by plants for their growth (Zörb et al., 2014; Basak et al., 2018; Ciceri et al., 2019). However, since several nutrients are abundant in the structure or interlayer sites of minerals, there is still a need to obtain more data on the release of other macro- (calcium, magnesium, and silicon) and micronutrients (manganese, boron, zinc, nickel, copper, and iron) during the dissolution of different minerals.

To predict the availability of nutrients from rocks, it is necessary to identify the present minerals, particularly those that may be dissolved quickly in the soil due to rhizosphere activity and that show adequate amounts of nutrients for plant growth; for this, chemical extractants have been used (Li et al., 2014; Basak, 2019). Other methods are still under development, especially since, currently, no single extractant can be used to determine nutrient availability and release rates as rocks are heterogeneous. An interesting alternative is to test the availability of nutrients from ground rocks, such as biotite micas, through plant-based extraction, which, when carried out successively, may indicate dissolution patterns and nutrient availability over time.

The objective of this work was to evaluate the nutrient availability for corn (*Zea mays* L.) when grown successively in pure and ground biotite schist and biotite syenite rock samples.

Materials and Methods

The rocks used for the experiment were biotite schist (BSC) and biotite syenite (BSY), collected in two Brazilian states, respectively: Goiás, from residue piles in quarries (Navarro et al., 2013b); and southeastern Bahia (Cruz et al., 2016). The cone-and-quartering reduction method was used to homogenize the air-dried samples. This procedure was repeated several times to ensure the complete homogenization

of the material, forming the bulk samples. Then, the samples were wet sieved to obtain four size fractions: < 53, 53–300, 300–1,000, and > 1,000 μm (Table 1).

To analyze the main chemical elements of BSC and BSY, the multi-acid solution method was used to digest 500 mg of each sample in 10:15:10:5 mL $HCl:HNO_3:HF:HClO_4$. The minor elements in this solution were analyzed through inductively coupled plasma optical emission spectrometry (ICP-OES) via the Avio 560 Max fully simultaneous ICP-OES instrument, with a built-in high throughput system for fast multilemental analyses (Perkin Elmer, Waltham, MA, USA), which were carried out at a laboratory of SGS Geosol Laboratórios Ltda. To determine the major elements, 0.8 g of each sample was mixed with 4.5 g lithium tetraborate flux and fused in Pt-5% gold crucibles, at 1,120°C, and then placed on fused glass discs, with 40 mm in diameter, being analyzed in the PW2400 wavelength dispersive X-ray fluorescence spectrometer (Philips, Amsterdam, the Netherlands). The loss on ignition was calculated after the samples were, respectively, heated overnight at 105°C to remove water and calcined at 1,000°C for approximately 2 hours.

The mineralogical composition of the BSC and BSY fractions < 53 μm was analyzed at the Mineral Laboratory of Universidade Federal do Pará by X-ray diffraction using the Empyrean diffractometer (Malvern Panalytical Ltd., Malvern, United Kingdom), with the powder method in the range of 5º < 2θ < 75º. CoKα radiation (40 kV; 40 mA) was applied, and the 2θ scanning speed was set at 0.02º s^{-1}. Data were obtained by the X'Pert Data Collector, version 4.0 software, and then treated on the X'Pert HighScore, version 3.0, software (Malvern Panalytical Ltd., Malvern, United Kingdom). To identify the minerals, the generated diffractogram was compared with the database of International Center for Diffraction Data (ICSD) (Gates-Rector & Blanton, 2019).

The Rietveld refinement was performed using the HighScore Plus, version 4.7, software (Malvern Panalytical Ltd., Malvern, United Kingdom). For quantitative determination of the mineralogical composition in each size fraction of BSC and BSY samples, the structural models (CIF files) for the identified mineral phases were obtained from the ICSD database. All phases of refinement include a scale factor, background polynomial function, and unit cell parameters. The W parameter of Caglioti's equation is refined only for the main phases, followed by V and U. For chlorites and micas, which show a strong preferred orientation, the (001) direction must be refined, and, for feldspars, such as microcline and albite, the (100) planes; atomic positions, however, were not refined in the present study.

The availability of nutrients from the rock powders for corn plants was evaluated using seeds from the 30F53VYHR hybrid (Pioneer, Corteva Agriscience do Brasil LTDA, Guarulhos, SP, Brazil), planted in 500 mL pots containing the bulk samples of BSC or BSY, in a split-plot design in time, under greenhouse conditions. Seven sets of four pots were prepared to allow seven successive cultivations (growth cycles) with destructive samplings, i.e., the seven sets of pots were reduced to only one set from the first to the seventh cycle. In every set, three (replicates) pots were kept with two corn plants and one without any, as a control treatment. Each pot was watered with deionized water every 1–2 days and fertilized with a nutrient solution containing 92.76 mg $NH_4H_2PO_4$ on the fifteenth and thirtieth day of each successive growth cycle.

The corn plants were grown for 45 days after emergence for an intensive interaction between plants and the rock samples. At the end of each cycle, whole plants from all pots were harvested. After the roots were thoroughly rinsed with distilled water, the harvested plants were oven dried, at 65°C, for 72 hours to obtain dry biomass (roots + shoots). Major-

Table 1. Particle size distribution of the crushed rock powders used in the experiment.

Sample	Particle size distribution (μm)				Total
	< 53	53–300	300–1,000	>1,000–2,000	(g per pot)
	--(%)--				
Biotite schist	21.1	17.4	2.4	59.1	546.82
Biotite syenite	11.9	23.2	29.6	35.3	681.02

(K, Ca, Mg, and Al) and minor elements (B, Cu, Fe, Mn, and Zn) were extracted by HNO_3:$HClO_4$ in a digestion block (Teixeira et al., 2017) and identified by ICP-OES. Moreover, for laboratory analyses, the rock content from one set of four pots was removed from the greenhouse after each one of the seven successive cycles. The remaining sets were re-sown for a new growth cycle.

The offtake of elements throughout the cycles was modeled using equations selected by the analysis of variance and then tested for normality (Shapiro-Wilk) and constant variance (homoscedasticity). The offtake of Fe and Al, extracted by plants from BSC and BSY, was correlated to the normalization of both elements by the sum of K, Ca, and Mg. All statistical analyses were performed using the Sigma Plot, version 12.0, software (Systat Software, Inc., San Jose, CA, USA).

The minerals within the rock samples were identified through electron probe microanalyses carried out in the Geosciences Institute of Universidade de Brasília using the JXA-8230 superprobe (JEOL, Akishima, Tokyo, Japan), coupled with five spectrometers and one energy dispersive detector (EDS), operating with 10 nA of current and 15 kV. The acquisition time was 10 s at the peak and 5 s at the background, with a beam diameter of 1.0 μm. The instrument was calibrated using natural and synthetic primary standards, and the resulting data were processed to calculate the structural formulas of the mineral phases. For the analyses of biotite, a total of 25 crystals of the mineral were used – 11 from BSC and 14 from BSY.

The samples were also characterized morphologically at Embrapa Agroenergia by scanning electron microscopy (SEM), using the SIGMA HV Zeiss field emission microscope with the InLens detector (Carl Zeiss Microscopy GmbH, Jena, Germany). A 10 nm thin conductive layer of gold was deposited over the samples using the Q150T-ES pumped coater for sputtering of oxidizing minerals (Quorum Technologies, Laughton, East Sussex, United Kingdom). Then, the chemical composition of the selected mineral particles was evaluated by energy-dispersive X-ray spectroscopy.

Results and Discussion

The chemical and mineralogical composition of the bulk samples and particle size fractions showed that the biotite mineral was present in both BSC and BSY (Figure 1 and Tables 2 and 3). Biotite has a significantly high Si and Al content and is the main active mineral prone to release nutrients, such as K, during the weathering of the two studied rocks (Table 3 and Figure 2). Since biotite is a subgroup of the mica group and forms a solid solution series with the annite [K Fe_3 $AlSi_3O_{10}$ $(OH)_2$] and phlogopite [K Mg_3 $AlSi_3O_{10}$ $(OH)_2$] end members of Fe and Mg, respectively, variations in the concentrations of these elements in natural biotite and the substitution of several others in the octahedral and tetrahedral silicate sheets may lead to differences in weathering rates (Madaras et al., 2013; Li et al., 2015; Basak, 2019). Essington (2015) highlighted that Fe(II) oxidation is one of the main factors in primary mineral weathering.

The biotite from the BSC and BSY samples was classified as, respectively: annite, siderophyllite, and phlogopite, being chemically composed by $K_{0.817}$ $Ba_{0.005}$ $(Mg_{1.198}$ $Fe_{1.157}$ $Al_{0.415}$ $Ti_{0.088})$ $(Si_{2.845}$ $Al_{1.154}$ $O_{11})$ $(OH_{1.97}$ $F_{0.02}$ $Cl_{0.001})$ (Navarro et al., 2013a); and only annite, a Fe-biotite usually composed by $K_{0.805}$ $Ba_{0.022}$ $Na_{0.011}$ $(Fe_{1.55}$ $Mg_{0.785}$ $Ti_{0.168}$ $Al_{0.255}$ $Mn_{0.01})$ $(Si_{2.963}$ $Al_{1.036}$ $O_{11})$ $(OH_{1.949}$ $F_{0.045}$ $Cl_{0.005})$ (Tischendorf et al., 2007). It should be noted that the stability of biotite decreases with an increasing Fe content, as the oxidation of structural Fe destabilizes the mineral (Malmström et al., 1995).

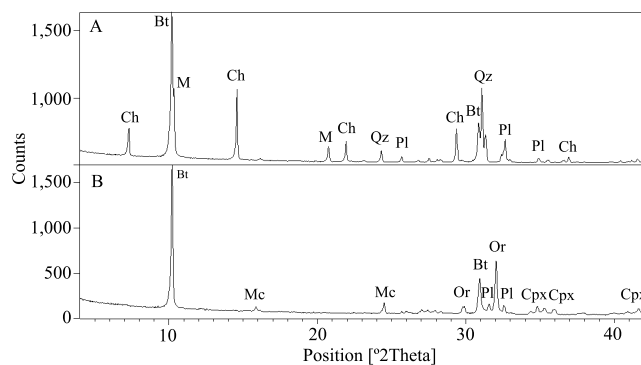Both rock bulk samples also contained other minerals of interest. In BSC, the following three

Figure 1. X-ray diffraction patterns of < 53 mm size particles of original samples of biotite schist and biotite syenite, evidencing, respectively: A, quartz (Qz), albite (Pl), biotite (Bt), muscovite (M), and chlorite (Ch); and B, orthoclase (Or), microcline (Mc), biotite (Bt), and clinopyroxene (Cpx).

stood out: albite [Na(Si₃Al)O₈], a plagioclase feldspar; chlorite, with the general chemical composition $(A,B)_{4-6}(Si,Al)_4O_{10}(OH,O)_8$, where A and B represent ions that may include Fe^{2+}, Fe^{3+}, Mg^{2+}, Mn^{2+}, Ni^{2+}, Zn^{2+}, Al^{3+}, Li^+, or Ti^{4+}; and muscovite, another K-bearing mineral composed by [KAl₂(AlSi₃O₁₀) (OH,F,Cl)₂]. Although all three are 2:1 phyllosilicate minerals, biotite and muscovite present interlayers with K^+ cations, whereas chlorite has a Mg-rich and brucite/gibbsite-like hydroxyinterlayer. The composition of the different interlayers is important since the expansion of the distance between them – due to the exchange

of nonhydrated K^+ by hydrated ions or the formation of hydroxypolymer interlayers – represents the start of the plant-induced transformation of biotite during weathering (Malmström et al., 1995). According to those authors, the amount and oxidation of Fe(II) significantly affect the susceptibility of chlorite to weathering, as also observed for biotite, whereas muscovite shows a greater resistance to alterations due to its high Al content. These results are indicative that Fe oxidation is one of the main components responsible for plant-induced mineral weathering.

Table 2. Chemical composition of the biotite schist and biotite syenite powders (bulk sample and fractions) determined by X-ray fluorescence spectrometry and inductively coupled plasma optical emission spectrometry at a laboratory of SGS Geosol – Laboratórios Ltda.[1].

Fraction (µm)	SiO₂	Al₂O₃	Fe₂O₃	CaO	MgO	TiO₂	P₂O₅	Na₂O	K₂O	MnO	BaO	Cr₂O₃	Cu	Mo	Zn	LOI[1]
						(%)							(mg kg⁻¹)			
						Biotite schist										
< 53	59.6	16.1	8.06	2.31	3.84	1.08	0.29	2.57	2.61	0.06	0.06	0.02	104	<3	104	2.18
53–300	59.7	19.0	7.74	0.87	3.68	0.57	0.15	1.84	4.14	0.05	0.11	0.02	35	<3	35	2.72
300–1,000	67.1	14.4	6.49	1.31	2.38	0.94	0.13	2.23	2.38	0.11	0.05	0.01	73	<3	73	1.59
>1,000	66.4	15.1	7.22	1.54	2.55	0.83	0.17	2.21	2.53	0.16	0.06	0.01	53	<3	53	1.5
Bulk sample[2]	62.6	16.8	7.8	1.44	3.2	0.86	0.2	1.93	3.19	0.12	0.07	0.02	49	<3	49	2.17
						Biotite syenite										
< 53	53.4	14.6	10.5	3.38	2.16	2.31	0.61	1.49	9.36	0.17	0.58	0.01	88	<3	88	1.28
53–300	53.7	14.9	11.1	2.69	2.14	2.32	0.38	1.19	10.70	0.14	0.58	0.01	46	<3	46	0.37
300–1,000	57.3	16.1	8.51	1.63	1.72	1.29	0.19	1.15	11.90	0.11	0.58	<0.01	35	<3	35	0.36
>1,000	57.6	16.0	7.41	1.89	1.54	1.26	0.24	1.38	11.80	0.11	0.6	<0.01	32	<3	32	0.29
Bulk sample[3]	55.9	16.0	8.16	2.00	1.70	1.49	0.24	1.19	11.30	0.11	0.57	<0.01	31	<3	31	0.49

[1]Loss on ignition. [2]Original sample.

Table 3. Mineralogical composition of the biotite schist and biotite syenite rock powders (bulk samples and fractions) used in the experiment.

Sample	Fraction (µm)	Quartz	Albite	Biotite	Muscovite	Chlorite	Clinopyroxene
	< 53	30.8	27.5	9.3	18.6	11.7	2.0
	53–300	33.4	22.2	10.3	22.5	10.5	1.1
Biotite schist	300–1,000	38.7	20.7	7.5	17.0	14.4	1.6
	>1,000	36.0	24.9	9.2	15.4	13.2	1.3
	Bulk sample[1]	35.7	22.1	11.2	17.9	11.3	1.7
		K-feldspar[2]	Albite	Biotite	Amphibole	Clinopyroxene	
	< 53	60.3	13.9	10.7	1.9	13.2	
	53–300	52.5	11.0	22.5	4.4	9.4	
Biotite syenite	300–1,000	55.2	13.7	15.5	5.0	10.7	
	>1,000	64.8	15.7	10.1	2.4	7.0	
	Bulk sample[1]	58.1	9.3	15.4	3.6	13.5	

[1]Original sample. [2]Orthoclase and microcline.

In BSY, the orthoclase and microcline alkaline K-feldspar minerals were the most abundant, with the general chemical formula $KAlSi_3O_8$. Other identified minerals of interest were albite and clinopyroxene; the latter is a mafic silicate of a subgroup of the pyroxenes, with the general chemical formula $ABSi_2O_6$, where $A = Ca^{2+}$, Na^+, and Li^+; and $B = Mg^{2+}$, Fe^{2+}, Fe^{3+}, and Al^{3+}. Amphibole, which may contribute to plant growth, was also found in small concentrations, with the general formula $A_{0-1}B_2C_5T_8O_{22}$ $(OH,F)_2$, where $A = Na^+$, K^+;

$B = Ca^{2+}$, Na^+, Mg^{2+}, Fe^{2+} and also Mn^{2+}, Li^+; $C = Mg^{2+}$, Fe^{2+}, Al^{3+}, Fe^{3+} and also Mn^{2+}, Zn^{2+}, Cr^{3+}, Li^+, or Ti^{4+}; and $T = Si$, Al. Although biotite content was similar in both bulk samples (Table 3), BSY showed 3.5 times more total K_2O than BSC (Table 2), probably because 52.5–64.8% of the rock is composed by K-feldspar, a mineral with a high structural stability, and also by albite, whose structure may include the substitution of Na by K. However, the total content of K may not reflect its availability for plant uptake in the short-term
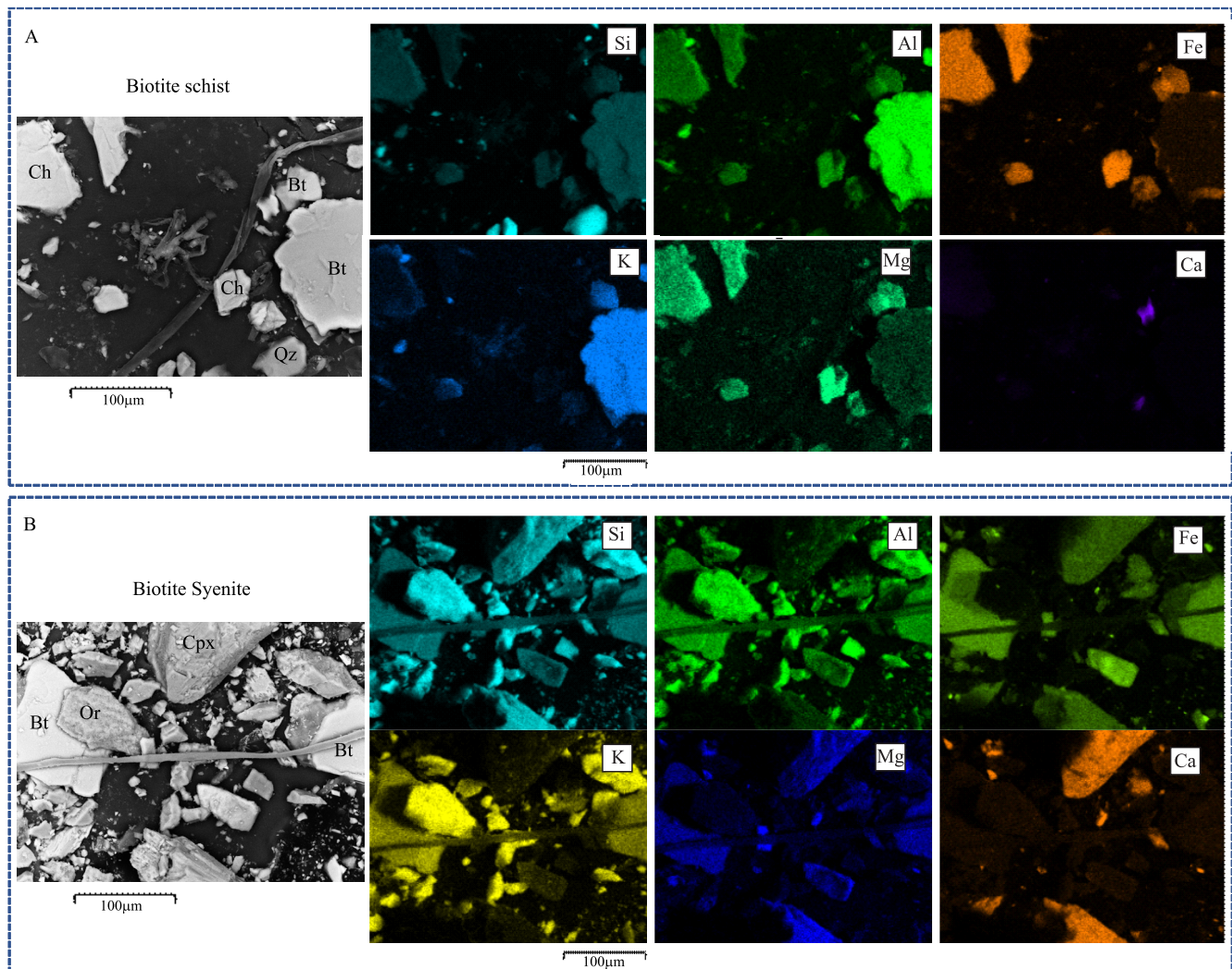

Figure 2. Images obtained by energy-dispersive X-ray spectroscopy (EDS) of the biotite schist and biotite syenite compounds close to the corn (*Zea mays*) root after the seventh growth cycle, showing the secondary electrons of: A, the biotite schist sample, evidencing light-colored quartz (Qz), biotite (Bt), and chlorite (Ch); and B, the biotite syenite sample, evidencing orthoclase (Or), biotite (Bt), and clinopyroxene (Cpx). Si, silicon; Al, aluminum; Fe, iron; K, potassium; Mg, magnesium; and Ca, calcium.

since a great amount of the element is locked in the muscovite structure of BSY.

Of the bulk samples, BSC improved corn plant growth, increasing the accumulated biomass in 15.3% (Figure 3). However, for both BSC and BSY, dry matter production was higher in the first growth cycle, accounting, respectively, for 23.9 and 20.7% of the total accumulated throughout the seven cycles, decreasing in each successive cycle.

After each cycle, a linear decrease in the pH was observed in the rock substrates, which is partially attributed to the increase in the weathering rate induced by the corn plants ($pH_{BSC} = 7.49^{**} - 0.22^{**}$(cycle), $R^2 = 0.91$; $pH_{BSY} = 7.93^{**} - 0.36^{**}$ (cycle), $R^2 = 0.88$). The main reasons for the decrease in pH were the removal of bases (especially Ca, Mg, and K) by the plants, the acidification caused by the applied rates of ammonium phosphate, the decomposition of the remaining roots,
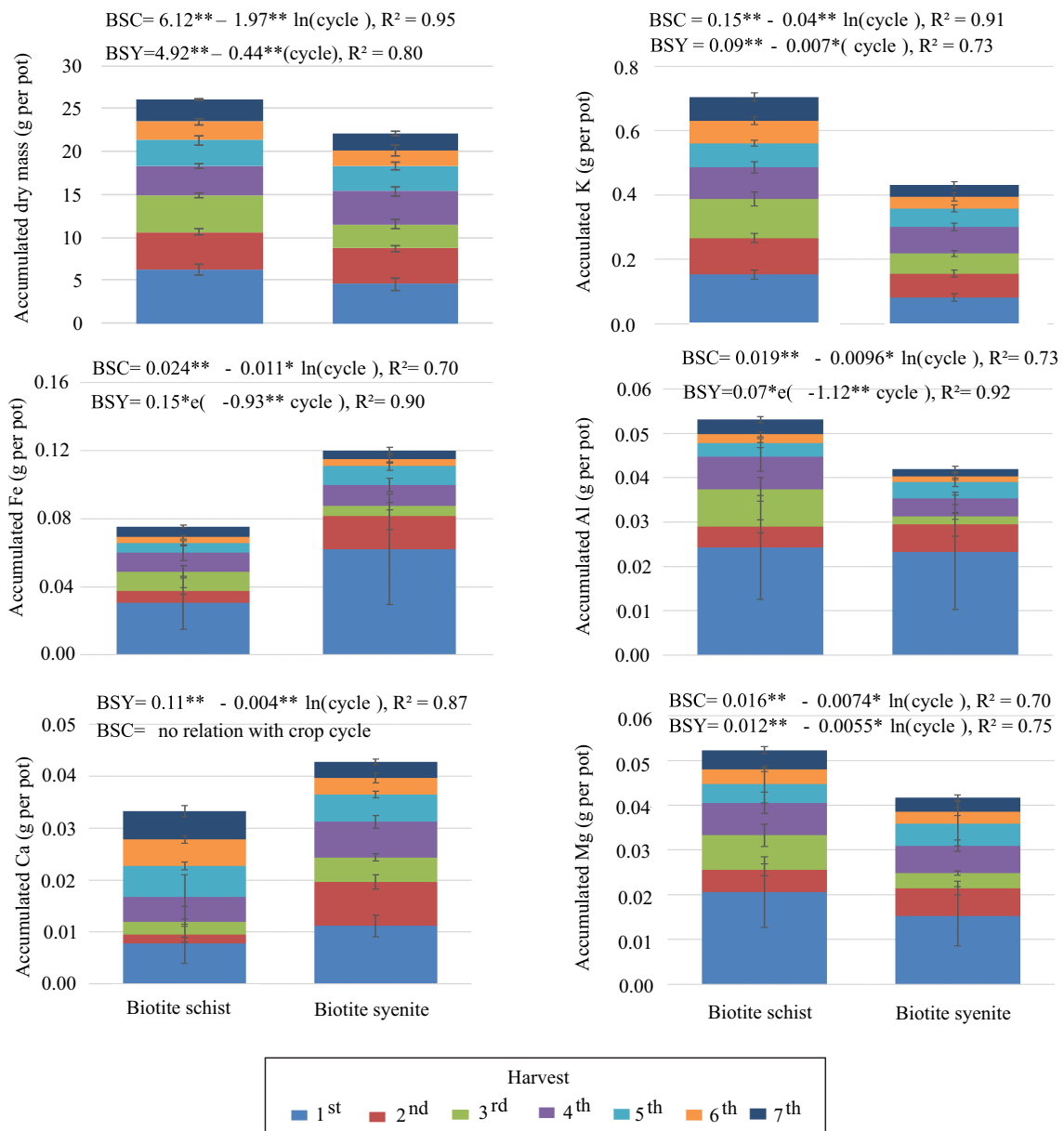

Figure 3. Dry mass and elements accumulated by corn (*Zea mays*) cultivated in biotite schist (BSC) and biotite syenite (BSY) powders after seven plant growth cycles. Bars in the center of the columns represent the standard error.

L.L. Krahl et al.

the substances released by the roots, the interaction between microorganisms, and the dissolution of atmospheric CO_2 into the pot solution (Li et al., 2017). Contrarily, the pH of the control samples did not change significantly, with a standard deviation of 8.02, 0.25 for BSC and of 7.85, 0.25 for BSY throughout the seven evaluated cycles.

In BSC and BSY, the concentrations of K in the dry mass of the corn plants ranged from 18.4 to 36 g kg^{-1} and from 13.9 to 26.5 g kg^{-1}, respectively. The offtake of the element by the plants was higher in the first cycle and lower in the last one, decreasing from 21.7 to 10.4% and from 18.9 to 8.5%, respectively, in BSC and BSY, corresponding to 0.15 and 0.07 g K per pot and to 0.08 and 0.03 g K per pot (Figure 3).

In both BSY and BSC, the content of Fe_2O_3 increased in the smaller-sized fractions due to a sort of segregation during fractionation (Table 2), which is related to an increase in biotite in the < 300 mm fractions as a result of preferential segregation during the milling process. According to Harley & Gilkes (2000), Bray et al. (2015), and Basak (2019), the reactivity of BSC is higher in finer fractions, especially in those <53 μm. Murakami et al. (2004) added that a higher structural concentration of Fe(II) and also of Mg accelerates the alteration and release of K from biotite, facilitating the formation of secondary minerals, as hydrobiotite and vermiculite, at least in an early stage. However, considering that vermiculite dissolves at a much slower rate than biotite, the dissolution rate of Mg-rich biotite (such as that found in BSC) is slower than that of Fe-rich biotite (as that in BSY). When the biotite has a high concentration of Fe, after the element is released into the solution, it is precipitated on particle surfaces, decreasing biotite weathering and K-release rates.

The content of Fe and Al accumulated in plants was higher in the first cycle (Figure 3), suggesting an initial and congruent dissolution of the fine and low crystallinity minerals, leading to the release of their elements into the solution. However, there was a reduction in the easily weatherable mineral surfaces since the offtake of Fe and Al from BSC and BSY by the corn plants decreased throughout the cycles. Data of the offtake of Fe and Al was normalized by the sum of K, Ca, and Mg, in order to observe how the latter elements influence the uptake rate of the former by the plants (Figure 4). The Fe content in BSY, as shown by the steep curve in the created graphs, was higher than

that in BSC over the cycles as affected by the sum of K, Ca, and Mg. However, Fe and Al offtake was positively correlated in both rocks by Pearson's correlation ($r_{BSC} = 0.99$ and $r_{BSY} = 0.99$; p<0.05), showing a similar trend. This strong correlation is indicative that the origin of Al offtake was a same mineral or group of minerals containing oxidizable Fe, i.e., biotite and chlorite in BSC and biotite and clinopyroxene, to a larger and lower extent, respectively, in BSY.

In BSY, clinopyroxene presents Fe and Mg, as well as a high and low content of Ca and Al, respectively, according to the analysis in the EDS (Figure 2). Since this mineral may be easily weathered depending on milling size and environmental conditions, it may become a source of Fe, Ca, and Mg for crops after applied to agricultural soils.

In BSC and BSY, Ca concentration in the dry mass of corn ranged, respectively, from 2.69 to 0.01 g kg^{-1} and from 2.8 to 1.4 g kg^{-1} throughout the cycles (Figure 3). This difference may be attributed to the fact that BSY presents a Ca-rich clinopyroxene, as shown by the EDS (Figure 2). Therefore, in BSC, the concentration of Ca was very low and the offtake data of this element by plants was a dispersion, showing no relationship with the growth cycle (Figure 3).

Contrastingly, in BSC, Mg content was higher, mainly in biotite and chlorite, as evidenced in the EDS images (Figure 2). In BSY, although the weathering of biotite and clinopyroxene also resulted in a significant amount of Mg, the availability of this element for corn plants decreased over the cycles as the finer particles dissolved, presenting a congruent and linear dissolution (Schott et al., 1981), which reflected in the decrease of Mg offtake in the plant tissue (Figure 3). The congruent dissolution of the fine particles on the surface of this mineral was confirmed by the SEM images (Figure 5), as also reported previously by Manning et al. (2017) and Basak (2019). The non-weathered and original biotite samples from BSC and BSY were covered with fine particles, which were reduced significantly after the seven evaluated crop cycles.

In BSC and BSY, Mg concentration in the dry mass of the corn plants ranged from 5.6 to 0.7 and from 5.2 to 0.9 g kg^{-1}, respectively. This result is indicative that the powders of both rocks may be considered a source of this nutrient to the plants, which is essential in natural soils that show an overall Mg deficiency, such as those in the Brazilian Cerrado region. The data for

exchangeable Mg indicate that 89.8% of the samples would be classified as containing low concentrations of the element, considering the minimum recommended value of <0.5 cmol$_c$ dm^{-3} (Lopes & Guilherme, 2016).

Several micronutrients from both rocks – such as Mn, B, Cueseon, there was ain Mn, and Zn – were mobilized by the corn plants (Figure 6). This is in alignment with Burghelea et al. (2018), who pointed out that most elements from minerals, predominantly from those that are easily dissolved, are significantly mobilized by plants and associated microbiota.

In BSC, the Mn concentrations in corn dry mass were low, varying from 122.8 to 43.9 mg kg^{-1} (Figure 6). As observed for Fe, Mn also oxidizes either after

dissolved or within crystals, transforming the solid state diffusion of electrons in electron acceptors in the soil solution at the mineral surface (Gilkes & McKenzie, 1988). Still according to these authors, after oxidized, the element remains in the soil due to its extremely low solubility of 10^{-28} mol kg^{-1} at pH 7, acting as a secondary oxide.

In contrast, in BSY, the concentrations of Mn in plant dry mass were higher, ranging from 405.4 to 173.2 mg kg^{-1}. Despite these high amounts, no symptoms of Mn toxicity were observed in the plants. In addition, there was a decrease in Mn offtake from the first to the last cycle (Figure 6).
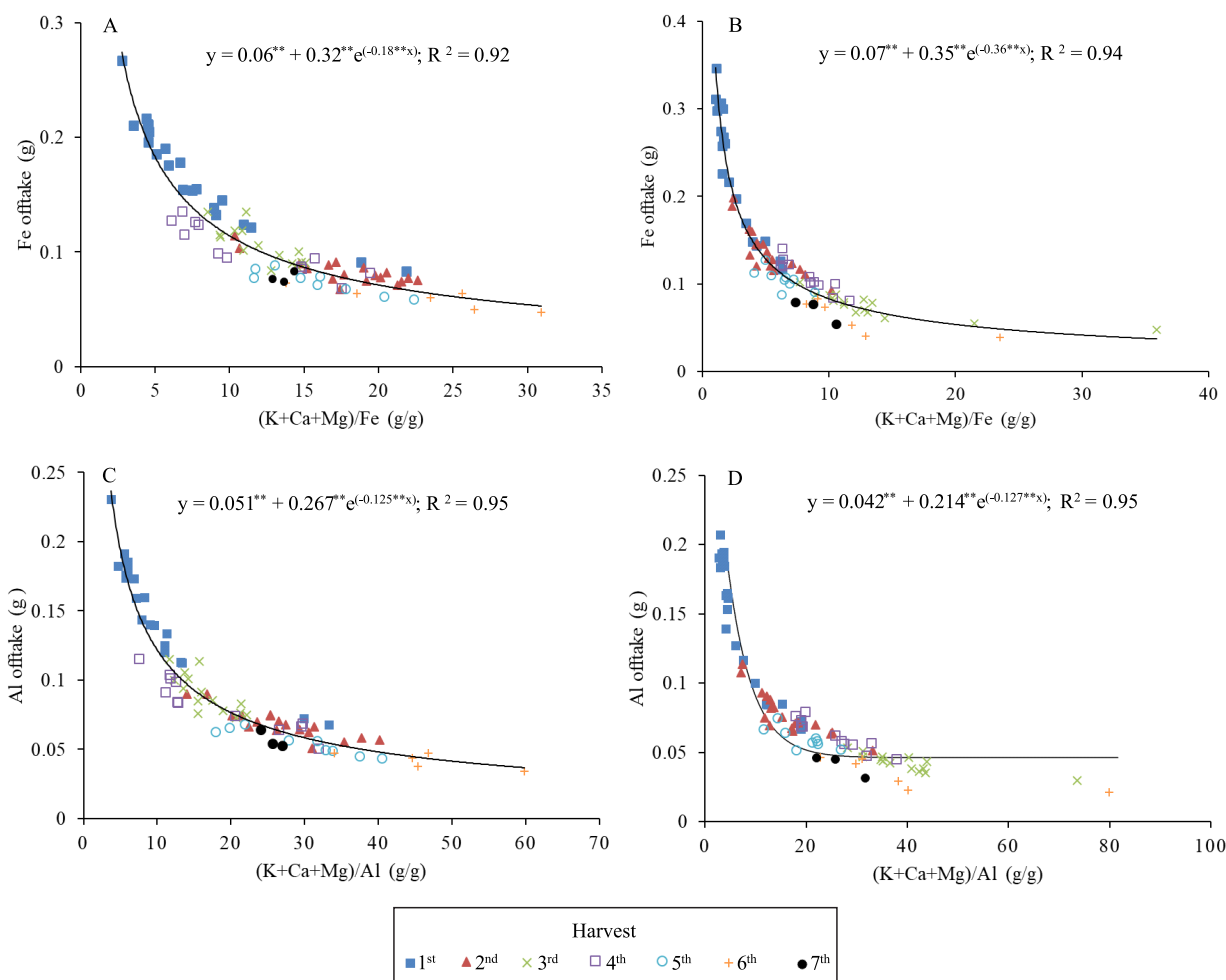

Figure 4. Offtake by corn (*Zea mays*) plants throughout seven growth cycles of: A and B, iron extracted from biotite schist and biotite syenite, respectively, as affected by the Fe normalized by the sum of potassium, calcium, and magnesium; and C and D, aluminum extracted from biotite schist and biotite syenite, respectively, as affected by the Al normalized by the sum of K, Ca, and Mg. **Significant at 1% probability.

Considering the other elements, plants showed lower B levels in BSC, with an almost constant offtake, ranging from 0.06 to 0.04 mg per pot throughout the experiment (Figure 6). Moreover, Cu concentrations decreased in corn dry mass from 26.1 to 7.0 and from 23.3 to 2.9 mg kg^{-1} in BSC and BSY, respectively, according to the used equation. The concentrations of Zn also decreased in the dry mass of the corn plants from 40.7 to 8.1 mg kg^{-1} in BSC and from 54 to 11.4 mg kg^{-1} in BSY, showing a decrease in Zn offtake from the first to the last plant cycle. According to Broadley

et al. (2012), the requirement of this nutrient for an optimal corn growth is 15–50 mg kg^{-1} Zn.

The obtained results are, therefore, indicative that the availability of nutrients from BSC and BSY was related to the oxidizable Fe content in the identified minerals – i.e., biotite, chlorite, and clinopyroxene, which are also rich in alkali and alkaline earth cations. However, the nutrients were not totally released to the plants since the dissolution of the rocks throughout the seven plant growth cycles was incomplete. This led to a decrease in the offtake of all elements by the plants, indicating that most of the small and easily weatherable particles
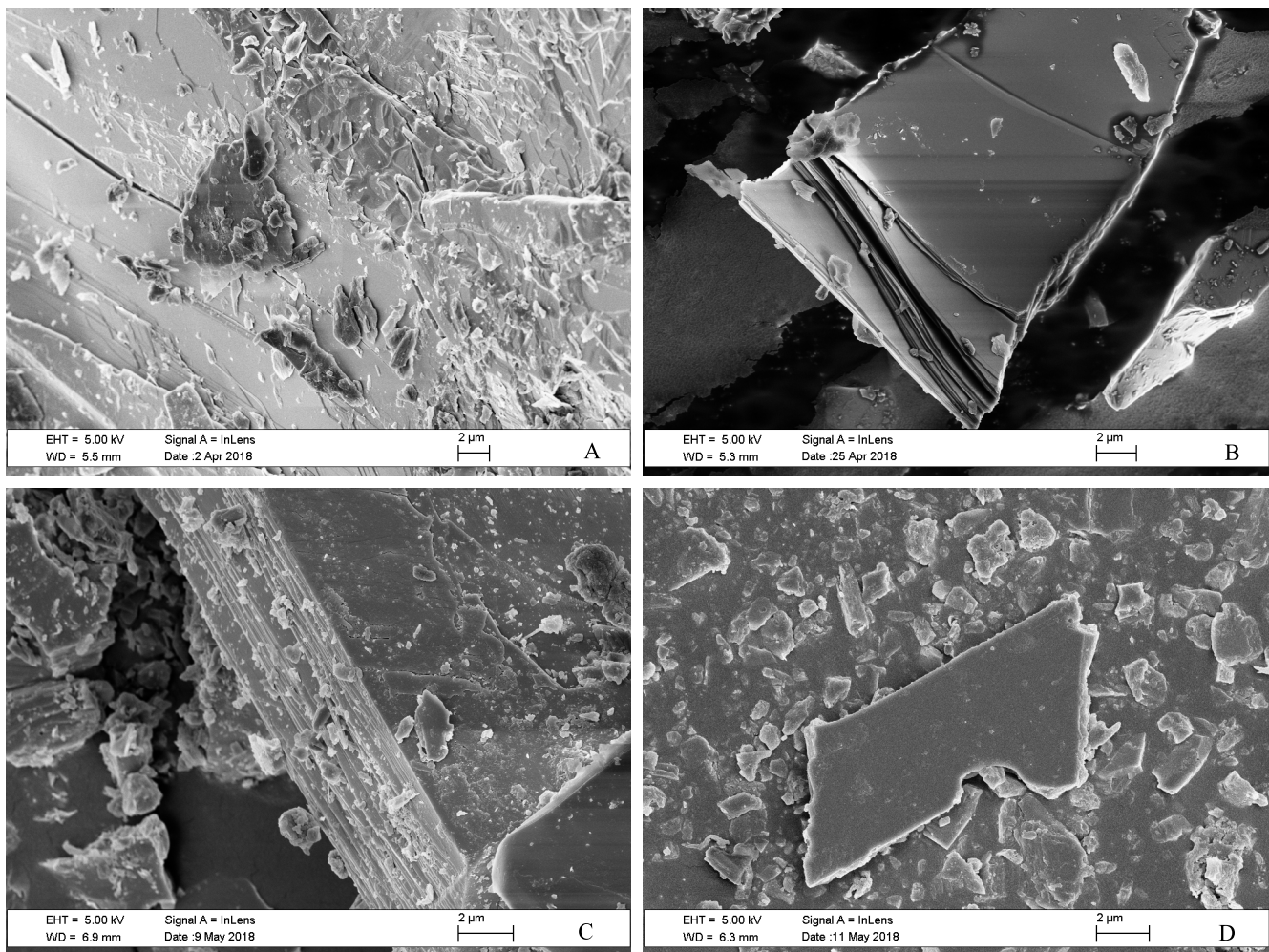

Figure 5. Images obtained by scanning electron microscopy of the biotite grains used in the corn (*Zea mays*) growth experiments, showing biotite surface: A and B, before and after plant growth in biotite schist, respectively; and C and D, before and after plant growth in biotite syenite, respectively.

and of the exposed surfaces of the minerals were congruently or incongruently dissolved. Consequently, both crushed rocks, through the dissolution of selected minerals, provided the plants with nutrients, whose contents decreased with time of cultivation. Despite this, the cultivated plants were still able to uptake several elements from BSC and BSY, including macro- and micronutrients essential for their growth.

It can be concluded, therefore, that corn plant growth is impaired in a small volume (500 mL) of pure and crushed rock due to the lower concentration and accumulation of released nutrients when compared with adequately corrected and fertilized soils. This is indicative that pure BSC and BSY rock powders are not an ideal substrate for plant growth. An alternative is mixing these rocks with soil for a more effective dissolution of the rock particles, which is expected to occur as soils are more biologically active and friable. This shows the importance of future studies on plant growth in substrates consisting of a mixture of rocks and soils.
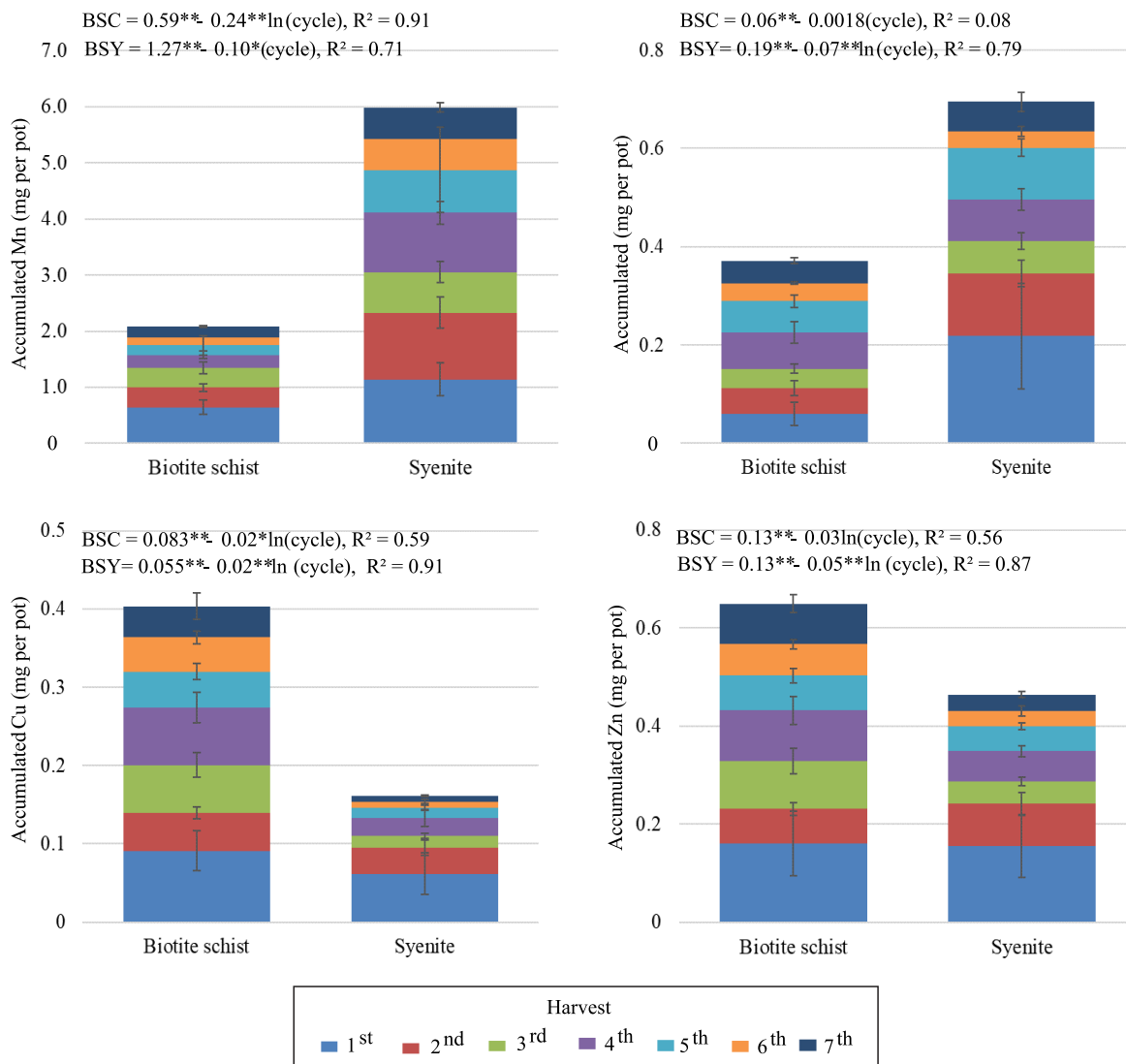

Figure 6. Offtake of accumulated micronutrients by corn (*Zea mays*) plants cultivated in biotite schist (BSC) and biotite syenite rock (BSY) powders after seven growth cycles. Bars in the center of the columns represent the standard error.

Conclusions

1. Pure and ground biotite schist and biotite syenite rock samples are sources of macro- and micronutrients for corn (*Zea mays*) plants.

2. Biotite schist releases more nutrients to plants grown in pure and ground rocks than biotite syenite.

3. The nutrient release rate from the mineral biotite relies on the content of magnesium and iron in the octahedral site.

Acknowledgments

References

BASAK, B.B. Waste mica as alternative source of plant-available potassium: evaluation of agronomic potential through chemical and biological methods. **Natural Resources Research**, v.28, p.953-965, 2019. DOI: https://doi.org/10.1007/s11053-018-9430-3.

BASAK, B.B.; SARKAR, B.; SANDERSON, P.; NAIDU, R. Waste mineral powder supplies plant available potassium: evaluation of chemical and biological interventions. **Journal of Geochemical Exploration**, v.186, p.114-120, 2018. DOI: https://doi.org/10.1016/j.gexplo.2017.11.023.

BRAY, A.W.; OELKERS, E.H.; BONNEVILLE, S.; WOLFF-BOENISCH, D.; POTTS, N.J.; FONES, G.; BENNING, L.G. The effect of pH, grain size, and organic ligands on biotite weathering rates. **Geochimica et Cosmochimica Acta**, v.164, p.127-145, 2015. DOI: https://doi.org/10.1016/j.gca.2015.04.048.

BROADLEY, M.; BROWN, P.; CAKMAK, I.; RENGEL, Z.; ZHAO, F. Function of nutrients: micronutrients. In: MARSCHNER, P. (Ed.). **Marschner's mineral nutrition of higher plants**. 3rd ed. Amsterdam: Elsevier, 2012. p.191-248. DOI: https://doi.org/10.1016/B978-0-12-384905-2.00007-8.

BURGHELEA, C.; ZAHARESCU, D.G.; DONTSOVA, K.; MAIER, R.; HUXMAN, T.; CHOROVER, J. Mineral nutrient mobilization by plants from rock: influence of rock type and arbuscular mycorrhiza. **Biogeochemistry**, v.124, p.187-203, 2015. DOI: https://doi.org/10.1007/s10533-015-0092-5.

BURGHELEA, C.I.; DONTSOVA, K.; ZAHARESCU, D.G.; MAIER, R.M.; HUXMAN, T.; AMISTADI, M.K.; HUNT, E.; CHOROVER, J. Trace element mobilization during incipient bioweathering of four rock types. **Geochimica et Cosmochimica Acta**, v.234, p.98-114, 2018. DOI: https://doi.org/10.1016/j.gca.2018.05.011.

CICERI, D.; ALLANORE, A. Local fertilizers to achieve food self-sufficiency in Africa. **Science of the Total Environment**, v.648, p.669-680, 2019. DOI: https://doi.org/10.1016/j.scitotenv.2018.08.154.

CICERI, D.; CLOSE, T.C.; BARKER, A.V.; ALLANORE, A. Fertilizing properties of potassium feldspar altered hydrothermally. **Communications in Soil Science and Plant Analysis**, v.50, p.482-491, 2019. DOI: https://doi.org/10.1080/00103624.2019.1566922.

CRUZ, S.C.P.; BARBOSA, J.S.F.; PINTO, M.S.; PEUCAT, J.-J.; PAQUETTE, J.L.; SOUZA, J.S. de; MARTINS, V. de S.; CHEMALE JÚNIOR, F.; CARNEIRO, M.A. The Siderian-Orosirian magmatism in the Gavião Paleoplate, Brazil: U-Pb geochronology, geochemistry and tectonic implications. **Journal of South American Earth Sciences**, v.69, p.43-79, 2016. DOI: https://doi.org/10.1016/j.jsames.2016.02.007.

ESSINGTON, M.E. **Soil and water chemistry**: an integrative approach. 2nd ed. Boca Raton: CRC PRESS, 2015. 656p.

GATES-RECTOR, S.; BLANTON, T. The powder diffraction file: a quality materials characterization database. **Powder Diffraction**, v.34, p.352-360, 2019. DOI: https://doi.org/10.1017/S0885715619000812.

GILKES, R.J.; MCKENZIE, R.M. Geochemistry of manganese in soil. In: GRAHAM, R.D.; HANNAN, R.J.; UREN, N.C. (Ed.). **Manganese in soils and plants**. Dordrecht: Kluwer Academic Publishers, 1988. p.23-35. DOI: https://doi.org/10.1007/978-94-009-2817-6_3.

HARLEY, A.D.; GILKES, R.J. Factors influencing the release of plant nutrient elements from silicate rock powders: a geochemical overview. **Nutrient Cycling in Agroecosystems**, v.56, p.11-36, 2000. DOI: https://doi.org/10.1023/A:1009859309453.

HINSINGER, P.; ELSASS, F.; JAILLARD, B.; ROBERT, M. Root induced irreversible transformation of a trioctahedral mica in the rhizosphere of rape. **European Journal of Soil Science**, v.44, p.535-545, 1993. DOI: https://doi.org/10.1111/j.1365-2389.1993.tb00475.x.

HINSINGER, P.; JAILLARD, B.; DUFEY, J.E. Rapid weathering of a trioctahedral mica by the roots of ryegrass. **Soil Science Society of America Journal**, v.56, p.977-982, 1992. DOI: https://doi.org/10.2136/sssaj1992.03615995005600030049x.

LI, J.; ZHANG, W.; LI, S.; LI, X.; LU, J. Effects of citrate on the dissolution and transformation of biotite, analyzed by chemical and atomic force microscopy. **Applied Geochemistry**, v.51, p.101-108, 2014. DOI: https://doi.org/10.1016/j.apgeochem.2014.10.001.

LI, T.; WANG, H.; WANG, J.; ZHOU, Z.; ZHOU, J. Exploring the potential of phyllosilicate minerals as potassium fertilizers using sodium tetraphenylboron and intensive cropping with perennial ryegrass. **Scientific Reports**, v.5, art.9249, 2015. DOI: https://doi.org/10.1038/srep09249.

LI, Z.; SU, M.; TIAN, D.; TANG, L.; ZHANG, L.; ZHENG, Y.; HU, S. Effects of elevated atmospheric CO_2 on dissolution of geological fluorapatite in water and soil. **Science of the Total Environment**, v.599-600, p.1382-1387, 2017. DOI: https://doi.org/10.1016/j.scitotenv.2017.05.100.

LOPES, A.S.; GUILHERME, L.R.G. A career perspective on soil management in the Cerrado region of Brazil. **Advances in Agronomy**, v.137, p.1-72, 2016. DOI: https://doi.org/10.1016/bs.agron.2015.12.004.

MADARAS, M.; MAYEROVÁ, M.; KULHÁNEK, M.; KOUBOVÁ, M.; FALTUS, M. Waste silicate minerals as potassium sources: a greenhouse study on spring barley. **Archives of Agronomy and Soil Science**, v.59, p.671-683, 2013. DOI: https://doi.org/10.1080/03650340.2012.667079.

MALMSTRÖM, M.; BANWART, S.; DURO, L.; WERSIN, P.; BRUNO, J. **Biotite and chlorite weathering at 25ºC**: the dependence of pH and (bi)carbonate on weathering kinetics, dissolution stoichiometry, and solubility; and the relation to redox conditions in granitic aquifers. Stockholm: Swedish Nuclear Fuel and Waste Management Co, 1995. 128p.

MANNING, D.A.C.; BAPTISTA, J.; LIMON, M.S.; BRANDT, K. Testing the ability of plants to access potassium from framework silicate minerals. **Science of the Total Environment**, v.574, p.476-481, 2017. DOI: https://doi.org/10.1016/j.scitotenv.2016.09.086.

MURAKAMI, T.; ITO, J.-I.; UTSUNOMIYA, S.; KASAMA, T.; KOZAI, N.; OHNUKI, T. Anoxic dissolution processes of biotite: implications for Fe behavior during Archean weathering. **Earth and Planetary Science Letters**, v.224, p.117-129, 2004. DOI: https://doi.org/10.1016/j.epsl.2004.04.040.

NADERIZADEH, Z.; KHADEMI, H.; AROCENA, J.M. Organic matter induced mineralogical changes in clay-sized phlogopite and muscovite in alfalfa rhizosphere. **Geoderma**, v.159, p.296-303, 2010. DOI: https://doi.org/10.1016/j.geoderma.2010.08.003.

NAVARRO, G.R.B.; ZANARDO, A.; CONCEIÇÃO, F.T. da. Metamorphic evolution and P-T path of gneisses from Goiás Magmatic Arc in southwestern Goiás State. **Brazilian Journal of Geology**, v.43, p.301-315, 2013a. DOI: https://doi.org/10.5327/Z2317-48892013000200008.

NAVARRO, G.R.B.; ZANARDO, A.; CONCEIÇÃO, F.T. da. O Grupo Araxá na região sul-sudoeste do Estado de Goiás. **Geologia USP. Série Científica**, v.13, p.5-28, 2013b. DOI: https://doi.org/10.5327/Z1519-874X2013000200002.

NOROUZI, S.; KHADEMI, H. Ability of alfalfa (*Medicago sativa* L.) to take up potassium from different micaceous minerals and consequent vermiculitization. **Plant and Soil**, v.328, p.83-93, 2010. DOI: https://doi.org/10.1007/s11104-009-0084-0.

SCHOTT, J.; BERNER, R.A.; SJÖBERG, E.L. Mechanism of pyroxene and amphibole weathering – I. Experimental studies of iron-free minerals. **Geochimica et Cosmochimica Acta**, v.45, p.2123-2135, 1981. DOI: https://doi.org/10.1016/0016-7037(81)90065-X.

TEIXEIRA, P.C.; DONAGEMMA, G.K.; FONTANA, A.; TEIXEIRA, W.G. (Ed.). **Manual de métodos de análise de solo**. 3rd ed. rev. e ampl. Brasília: Embrapa, 2017. 574p.

TISCHENDORF, G.; FORSTER, H.-J.; GOTTESMANN, B.; RIEDER, M. True and brittle micas: composition and solid-solution series. **Mineralogical Magazine**, v.71 p.285-320, 2007. DOI: https://doi.org/10.1180/minmag.2007.071.3.285.

WANG, J.G.; ZHANG, F.S.; CAO, Y.P.; ZHANG, X.L. Effect of plant types on release of mineral potassium from gneiss. **Nutrient Cycling in Agroecosystems**, v.56, p.37-43, 2000. DOI: https://doi.org/10.1023/A:1009826111929.

ZÖRB, C.; SENBAYRAM, M.; PEITER, E. Potassium in agriculture – status and perspectives. **Journal of Plant Physiology**, v.171, p.656-669, 2014. DOI: https://doi.org/10.1016/j.jplph.2013.08.008.